

This article was downloaded by: [Tomsk State University of Control Systems and Radio]

On: 17 February 2013, At: 06:01

Publisher: Taylor & Francis

Informa Ltd Registered in England and Wales Registered Number: 1072954

Registered office: Mortimer House, 37-41 Mortimer Street, London W1T 3JH, UK



## Molecular Crystals

Publication details, including instructions for authors and subscription information:

<http://www.tandfonline.com/loi/gmcl15>

## Space Charge Limited Currents in Polycrystalline p-Quaterphenyl Layers

A. Szymanski<sup>a</sup>

<sup>a</sup> Institute of Physics, Technical University of Łódź, Łódź, Poland

Version of record first published: 21 Mar 2007.

To cite this article: A. Szymanski (1968): Space Charge Limited Currents in Polycrystalline p-Quaterphenyl Layers, *Molecular Crystals*, 3:3, 339-355

To link to this article: <http://dx.doi.org/10.1080/15421406808083450>

PLEASE SCROLL DOWN FOR ARTICLE

Full terms and conditions of use: <http://www.tandfonline.com/page/terms-and-conditions>

This article may be used for research, teaching, and private study purposes. Any substantial or systematic reproduction, redistribution, reselling, loan, sub-licensing, systematic supply, or distribution in any form to anyone is expressly forbidden.

The publisher does not give any warranty express or implied or make any representation that the contents will be complete or accurate or up to date. The accuracy of any instructions, formulae, and drug doses should be independently verified with primary sources. The publisher shall not be liable for any loss, actions, claims, proceedings, demand, or costs or damages whatsoever or howsoever caused arising directly or indirectly in connection with or arising out of the use of this material.

## Space Charge Limited Currents in Polycrystalline *p*-Quaterphenyl Layers

A. SZYMAŃSKI

Institute of Physics, Technical University of Łódź, Łódź, Poland

*Received August 4, 1967; in revised form September 25, 1967*

**Abstract**—Measurements of space-charge limited currents have been made on evaporated thin films of organic compound *p*-quaterphenyl using metal electrodes. A study of current as a function of voltage and temperature indicated in layers examined the existence of an exponential trap level distribution. The new technique for evaluating the shape of trap level distribution was proposed.

The application of space charge limited current (SCLC) theory to studies of electrical conductivity of organic substances, not only has permitted a reasonable explanation of previously observed phenomena but also has augmented our knowledge of the electronic structure of the examined compounds.<sup>1</sup>

Many interesting parameters, characterizing the electronic structure of the examined dielectric such as the density and the distribution of the trap levels, the mobility of charge carriers, and the density of the carriers in the conduction band, have been evaluated<sup>2-8</sup> using methods based on SCLC theory.

The majority of the work cited above has been devoted to dielectrics containing shallow traps. Few papers<sup>3,9,10</sup> were concerned with the more troublesome problem—the dielectrics with deep and distributed trap levels. In this case, SCLC theory has predicted the important contribution of the shape of the trap level distribution in the current-voltage characteristics<sup>9,10</sup>.

In this paper, a comparison between the predictions of the theory and the results of SCLC studies in polycrystalline *p*-quaterphenyl (*p*-QPh) layers is presented.

### 1. Experimental

The dependence of current on temperature and applied voltage was measured in *p*-QPh layers. The material, *p*-QPh, was supplied by AG Fluka, puriss grade and was further purified by vacuum

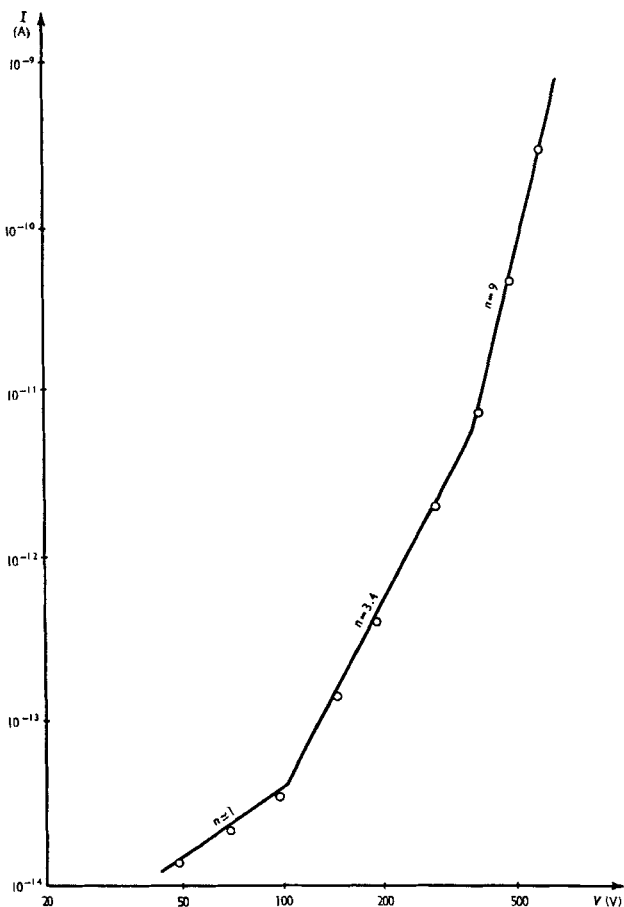


Figure 1. Dependence of the logarithm of dark current on the logarithm of voltage for *p*-quaterphenyl layers with gold electrodes. The thickness of the layer is 5  $\mu\text{m}$ . The temperature 300°K.

sublimation. The layers were obtained by vacuum sublimation from quartz containers in a vacuum of  $10^{-4}$  mm Hg, the temperature of the support being about 300°K. The layers were polycrystalline.

The dimensions of crystallites were  $0.3\text{--}1\text{ }\mu\text{m}$ . Metal electrodes (Au or Pt) were applied to the layers in the "sandwich" configuration by vacuum evaporation. Measurements of the current,

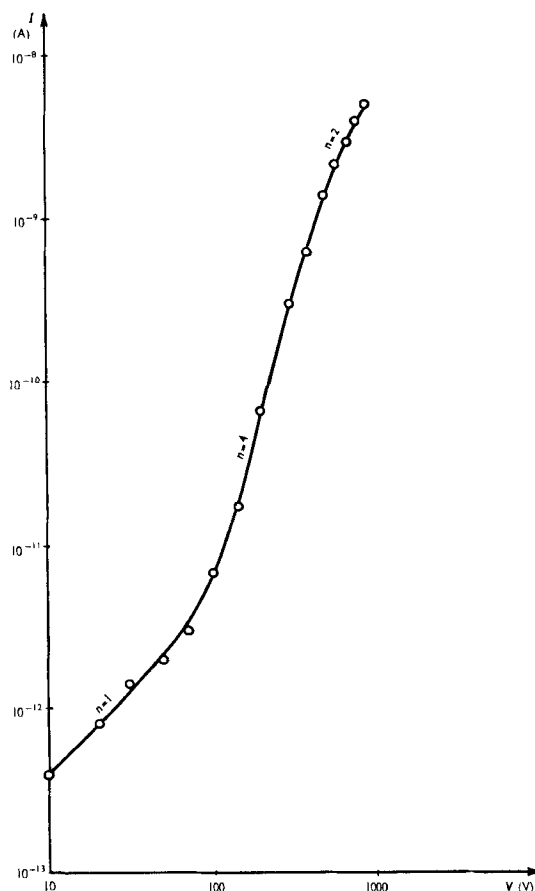


Figure 2. Dependence of the logarithm of dark current on voltage for *p*-quaterphenyl layers with Pt electrodes (Au-*p*-QPh-Pt). Thickness of the layer is  $6\text{ }\mu\text{m}$ , temperature  $300^\circ\text{K}$ .

temperature and voltage relationships were carried out in vacuum ( $10^{-4}\text{--}10^{-2}$  Tr) using a vibrating reed electrometer and an X-Y recorder. When the photocurrent had to be examined, the samples

were illuminated through the quartz window by the 365 nm Hg line isolated by an interference filter.

The measurement of current-temperature and voltage dependence were performed using the procedure proposed by Harnik,<sup>11</sup> based on current-temperature dependence measurements for a series of fixed voltages. The heating rate of the sample was so adjusted as to be smaller than the rate of the space charge relaxa-

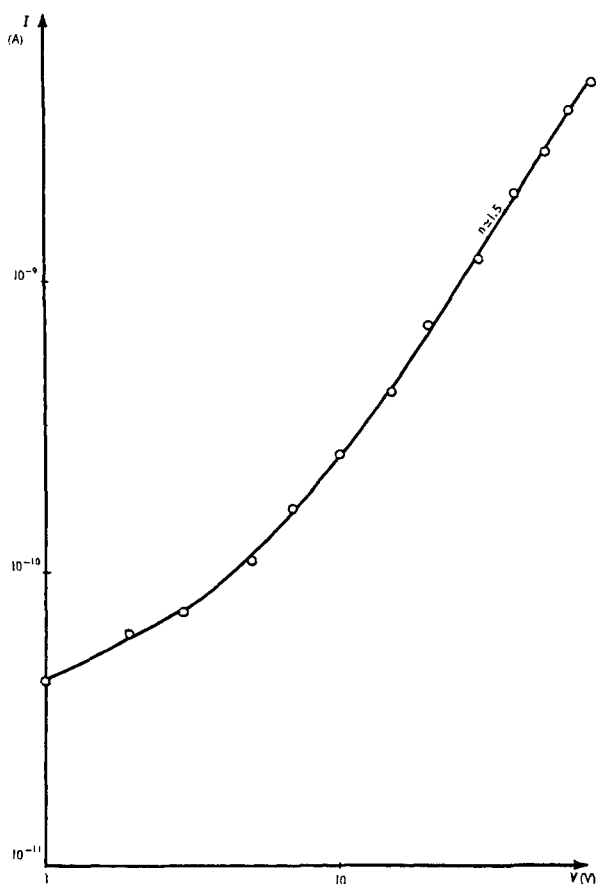


Figure 3. Dependence of the logarithm of photocurrent on the logarithm of voltage for the layer Au-*p*-QPh-Pt. Thickness of the layer 6  $\mu\text{m}$ , temperature 300°K.

tion process in the layer (the relaxation time was about  $10 \text{ s}^{12}$ ). The rate of heating or cooling was about  $0.01^\circ\text{K/s}$ . Because of the undesirable effects connected with thermal trap emptying during the heating process, the same measurement was also repeated during cooling of the sample. The current-temperature curves obtained during cooling were less disturbed than those obtained during the heating up of the sample.

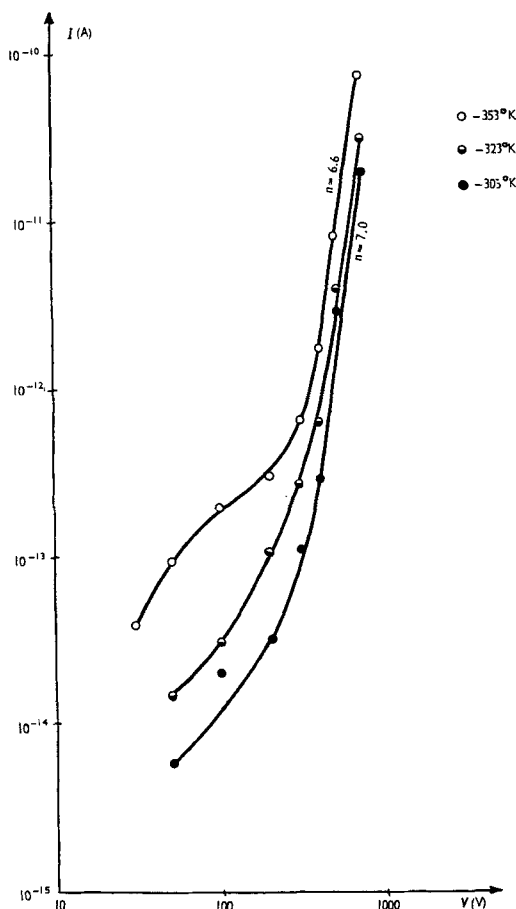


Figure 4. Dependence of the logarithm of dark current on the logarithm of voltage for the different temperatures. The layer Au-*p*-QPh-Au, thickness  $5 \mu\text{m}$ .

## 2. Results

The shape of the observed current-voltage characteristic depends on various factors: electrode material, range of the fields applied, intensity of illumination and temperature. The current-voltage characteristics drawn in a  $\log I$ - $\log V$  plot are presented in Figs. 1-5. It can be seen (Figs. 4 and 5) that increasing temperature has little influence on the shape of the curves, decreasing only the slope of the curves. Comparison of Figs. 2 and 3 shows that the

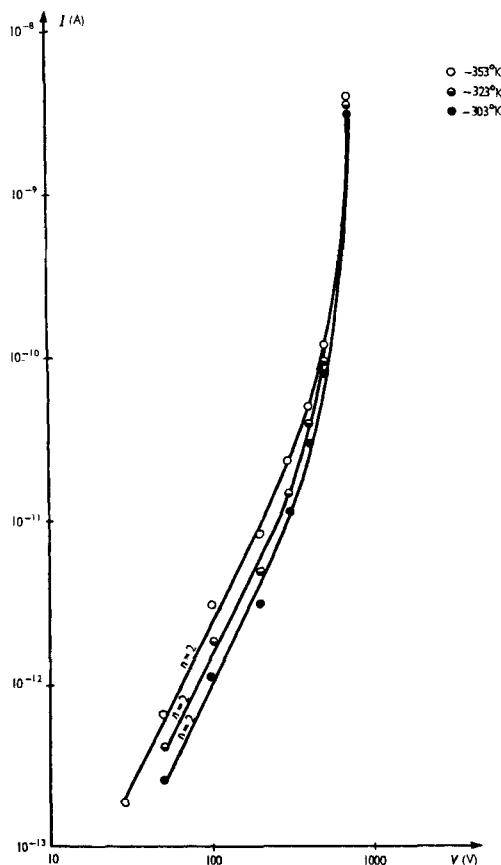


Figure 5. Dependence of the logarithm of photocurrent on the logarithm of voltage for different temperatures. The layer Au-*p*-QPh-Au, thickness 5  $\mu\text{m}$ .

shape of the curve for dark and photocurrent is not always the same. There are also differences between the shape of the curve for Au-(*p*-QPh)-Au and Au-(*p*-QPh)-Pt samples. These differences may originate both because of different electrode material and different properties of the sample.

In general, the characteristics drawn in the  $\log I$ - $\log V$  scale, are consistent with straight lines of different slope (Figs. 1-5). In the sample for which the current-voltage curves are presented in Figs. 4 and 5, dependence of the voltage on the thermal activation energy of the dark current ( $E_a$ ) and photocurrent ( $E_{pha}$ ) was measured. Data were calculated from  $I=f(T)$  curves obtained for the 300-353°K temperature range with the aid of the least squares method. The calculated values and the probable error are presented in Tables 1 and 2. Before using this method it was determined that  $\ln I$  was a linear function of  $1/T$ , and the extrapolation for the linear function was carried out.

TABLE 1 Values of Thermal Activation Energies of Dark Conductivity as a Function of Voltage

$V$ (volts)	30	50	100	200	300	400	500	700
$E_a$ (eV)	0.9	0.53	0.43	0.50	0.28	0.32	0.19	0.17
$\Delta E_a$ (eV)	0.2	0.14	0.09	0.15	0.15	0.10	0.05	0.03

TABLE 2 Values of Thermal Activation Energies of Photoconductivity as a Function of Voltage

$V$ (volts)	30	50	100	200	300	400	500	700
$E_a$ (eV)	0.19	0.24	0.16	0.18	0.13	0.09	0.08	0.05
$\Delta E_a$ (eV)	0.07	0.07	0.03	0.2	0.2	0.01	0.01	0.02

### 3. Interpretation

#### 3.1. RESULTS OF PREVIOUS THEORETICAL AND EXPERIMENTAL WORK

SCLC theory in dielectrics with continuous trap level distribution was developed by Rose,<sup>9</sup> Mark and Helfrich<sup>3</sup> and Muller.<sup>10</sup> The predicted slope of the current-voltage characteristics is dependent



on the assumed trap level distribution. For the trap distribution exponentially decreasing with energy (measured from the bottom of conduction band)

$$\rho(\epsilon) = \rho_0 \exp -\epsilon/kT_c \quad (1)$$

(where:  $\rho_0$  and  $kT_c$  are constant values, characteristic of the assumed trap level distribution,  $\epsilon$ —energy) the current density–voltage dependence<sup>3, 9, 10</sup> is given by the following equation:

$$I = \frac{e\mu_0 N_c}{L} \left( \frac{b}{N_T} \right)^{T_c/T} V^{[T_c/T+1]} \quad (2)$$

where:  $b = \frac{\alpha\beta\epsilon\epsilon_0}{eL^2}$ ;  $\epsilon\epsilon_0$ —dielectric constant,  $\alpha\beta$ —constant,  $\frac{1}{2} \leq \alpha\beta \leq 2$ ,  $e$ —electronic charge,  $N_T$ —number of the traps per unit volume,  $L$ —thickness of the layer,  $\mu_0$ —the mobility of the carriers in the conduction band,  $N_c$ —number of states in the conduction band (the SI—system of units was adapted). For the trap density exponentially increasing with energy

$$\rho(\epsilon) = \rho_0 \exp \frac{\epsilon - \epsilon_l}{kT} \quad (3)$$

$\epsilon_l$ —lower limit of the trap level distribution, the current density–voltage relation is given by:<sup>10</sup>

$$I = \frac{e\mu_0 N_c V}{L} [\exp -\epsilon_l/kT] \left[ 1 - \frac{bV}{\rho_0 kT_c} \right]^{-T_c/T} \quad (4)$$

Assumption of different trap level distributions would give different current–voltage relations, e.g. for the uniform trap level distribution:<sup>10</sup>

$$I \sim \exp(\text{const } V) \quad (5)$$

In the work of Mark and Helfrich<sup>3</sup> the characteristic energy  $kT_c$  of the trap level distribution was calculated from the slope of the  $\log I - \log V$  characteristic [ $n = T_c/T + 1$ ]. As has been shown previously,<sup>13</sup> in the case of overlapping maxima of the trap level distribution it is hard to find that part of the current–voltage characteristic properly described by Eq. (2). A more precise method of evaluation of  $kT_c$  energy consists of comparing the

experimentally determined dependence of the thermal activation energy on voltage [ $E_a = f(V)$ ]. The  $E_a$  values calculated from Eqs. (2) or (4) are respectively:

$$E_a = kT_c \ln \frac{N_T}{b} - kT_c \ln V - \frac{d}{d\left(\frac{1}{kT}\right)} \ln(N_c \mu_0) \quad (6)$$

$$E_a = \epsilon_i + kT_c \ln \left(1 - \frac{bV}{\rho_0 kT_c}\right) - \frac{d}{d\left(\frac{1}{kT}\right)} \ln(N_c \mu_0) \quad (7)$$

In the case in which the energy density of the traps decreases the  $E_a \sim \ln V$  dependence is a straight line. From the slope of this line the value  $kT_c$  is obtained easily. The assumption that the value of

$$\frac{d}{d\left(\frac{1}{kT}\right)} \ln(N_c \mu_0)$$

is equal to several  $kT$  and can be neglected compared to  $kT_c \ln(N_T/b)$  permits the calculation of the  $N_T$  value. For the trap density distribution given by Eq. (3) for  $bV/\rho_0 kT_c \ll 1$

$$E_a = \epsilon_i - \frac{b}{\rho_0} V - \frac{d \ln(N_c \mu_0)}{d\left(\frac{1}{kT}\right)} \quad (8)$$

Thus it is possible to calculate the  $\rho_0$  value only when  $\epsilon_i \gg kT$ . The task is more complicated, when the determined  $E_a$  value also contains the height of the electrode barrier  $\phi$  (the current is not fully space charge limited). In this case only the  $kT_c$  value can be calculated.

The second possible way of determining the trap density distribution<sup>13</sup> (without assuming the shape of the distribution) is based on the relation proposed by Rose<sup>9</sup>

$$\frac{CV}{eL} = \int_{\epsilon_f}^{\epsilon_{fo}} \rho(\epsilon) d\epsilon \quad (9)$$

when  $C$ —the capacity of the sample,  $\epsilon_{fo}$  and  $\epsilon_f$  the Fermi level positions for  $V=0$  and  $V$ , other symbols are previously described.

Differentiating over  $\epsilon_f$  one may obtain

$$\frac{C}{eL} \frac{dV}{d\epsilon_f} = \rho(\epsilon_f) \quad (10)$$

It can be easily shown<sup>8</sup> that in the case of pure SCLC

$$E_a = E_f - \frac{d}{d\left(\frac{1}{kT}\right)} \ln(\mu_0 N_c)$$

where

$$\left| \frac{d}{d\left(\frac{1}{kT}\right)} \ln(\mu_0 N_c) \right| \leq 2kT$$

so

$$\frac{C}{eL} \frac{dV}{dE_a} = \rho(E_a \pm nkT) \quad n \leq 2 \quad (11)$$

The trap level density distribution calculated from Eq. 11 may be shifted about  $2kT$  in the energy scale without disturbing the shape of the distribution. The electrical properties of *p*-terphenyl and *p*-quaterphenyl monocrystals were investigated by several authors.<sup>3, 14, 15</sup> A more detailed study was performed by Mark and Helfrich.<sup>3</sup> For the *p*-terphenyl monocrystals the density of traps, the energy  $kT_c$ , mobility  $\mu_0$  and the cross-section for trapping process  $S$  were measured. The  $\mu_0$  values [ $\mu_0 = 10^{-2}$  cm<sup>2</sup>/Vs] were obtained from the transient SCLC measurements, characteristic energy of the trap level distribution  $kT_c$  [ $kT_c = 0.05$  eV] from the slope of the  $\log I$ – $\log V$  curve,  $N_T$  [ $N_T = 3.4 \times 10^{16}$  cm<sup>-3</sup>] with the help of the Eq. (2), and the trapping cross-section  $S$  [ $S = 4 \times 10^{-17}$  cm<sup>2</sup>] from the decay of the current.

Several deep trapping levels or quasilinear distributions were also found<sup>16</sup> in *p*-quaterphenyl layers by the thermally stimulated current method [0.6–0.7 eV and also very probably 0.2 and 1 eV].

### 3.2. DETERMINATION OF TRAP LEVEL DISTRIBUTION

With the help of the Eqs. (6), (7) and (11) the parameters of the existing trap level density distribution were calculated. In Figs. 6 and 7 the dependence of  $E_a$  and  $E_{pha}$  on  $\log V$  is shown. Only  $E_a$

depends linearly (in the limits of error) on  $\log V$ . So, from Fig. 6 the calculated  $kT_c$  and  $N_T$  values are

$$kT_c = 0.18 \pm 0.02 \text{ eV}$$

$$N_T \simeq 10^{16} \text{ cm}^{-3}$$

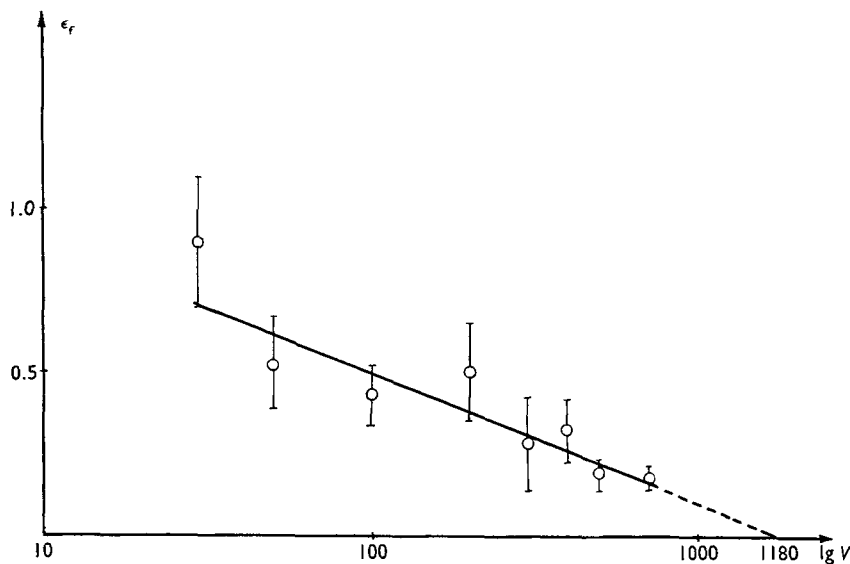


Figure 6. Dependence of thermal activation energy of dark conductivity on logarithm of the voltage.

In the high-voltage part of the graph given in Fig. 7 linear behavior can be assumed. The evaluated  $kT_c$  is between 0.05 and 0.09 eV.

The same distribution was calculated from Eq. (11) using the voltage  $E_a$  and  $E_{pha}$  dependence. Values representing the density of traps were obtained by substituting in relation 11;  $C = 10^{-9} \text{ F}$  and  $L = 5 \times 10^{-4} \text{ cm}$ . Values  $dV/dE_a$  were obtained graphically from the  $E_{a/pha}$  on  $V$  dependence. Final results are presented in Fig. 8. The procedure of graphical differentiation is arbitrary and can produce considerable errors, which can be minimized, when the shape of the curve is known.

In Fig. 8 the results of the calculations are plotted for both dark

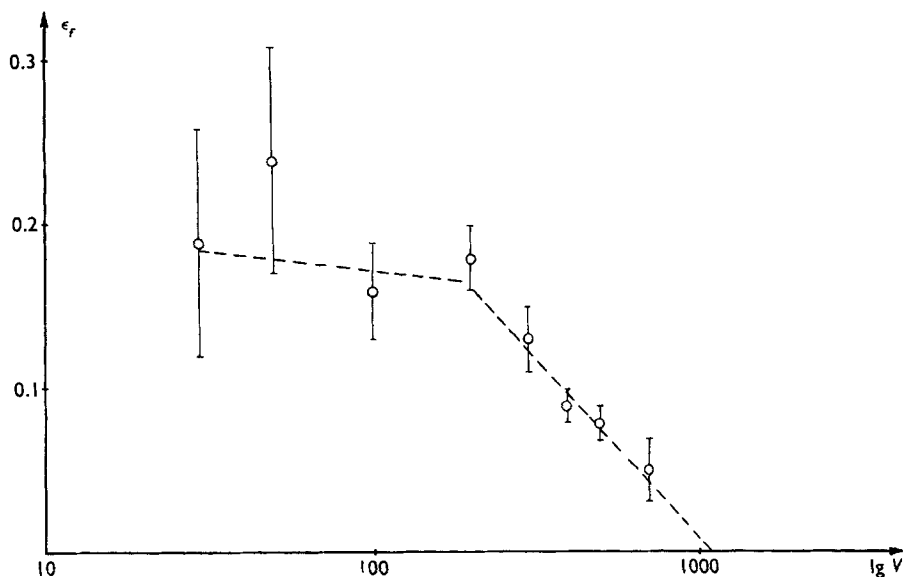


Figure 7. Dependence of thermal activation energy of photoconductivity on logarithm of the voltage.

current and photocurrent in spite of differences between these two processes, e.g. the more prominent role of recombination and the expected deviation from the unipolarity in the case of the photocurrent.

It should be stressed, that Eq. (9) contains restrictions to its application to bipolar currents. The procedure based on Eq. (11) may be more general than that making the use of Eqs. (6) and (7). The values of the depths and density of traps obtained from both methods and the thermally stimulated currents (TSC) are gathered in Table 3. Good agreement between values obtained by these methods is promising and suggest that they may yield reproducible results.

The slopes observed in Figs. 1 and 4 [ $n=9$ ;  $n=7$ ] may be also connected to the 0.2 eV maximum. The calculated shape of the trap distribution curve (Fig. 8) suggest the existence of a second maximum situated below 0.1 eV. The overlapping of these

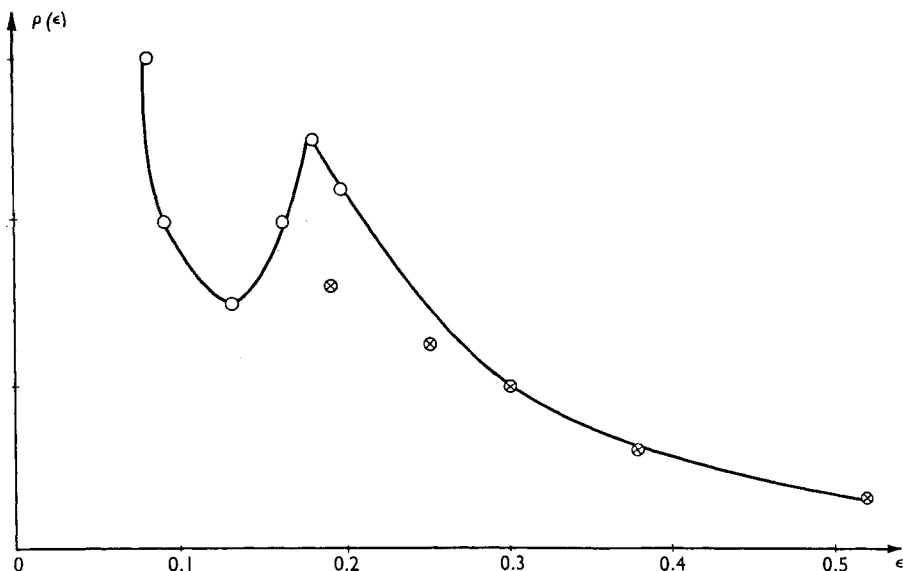


Figure 8. Trap density distribution determined from Eq. (11). The circles with the cross inside correspond to values calculated from the data presented in Table 1, the circles without crosses from Table 2.

TABLE 3 Trap Depth  $\epsilon_T$  and Density  $N_T$  Obtained from Different Methods

	$\epsilon_T$	$N_T$
SCLC Eq. (6)	$(kT_c) 0.18 \text{ eV} \pm 0.2 \text{ eV}$	$10^{16} \text{ cm}^{-3}$
SCLC Eq. (11)	$(\epsilon_{\max}) 0.17 \text{ eV}$	$\sim 10^{16} \text{ cm}^{-3}$
TSC	$(\epsilon_{\max}) 0.25 \text{ eV}$	$\sim 5 \times 10^{15} \text{ cm}^{-3}$

two maxima means that in the 0.1–0.2 eV range the trap level distribution is neither described by Eq. (1) nor Eq. (3) (Fig. 8).

### 3.3. THE SHAPE OF THE VOLTAGE-CURRENT CHARACTERISTIC

In organic dielectrics, for example, anthracene, the existence of several linear or quasilinear trap level distributions was observed.<sup>17,18</sup> As was shown in previous work,<sup>13</sup> the  $\log I$ – $\log V$  curve in that case is composed of linear regions with different

slopes. The lines with considerable slopes would be responsible for filling the corresponding maxima of the trap level distribution.

If the maxima are sufficiently separated it may be the case that the next one is situated in the low energy range where  $kT_c \simeq kT$ . Then following Muller<sup>10</sup> the current-voltage relation ought to be the same as in the case of shallow traps.

$$I = \epsilon \epsilon_0 \alpha^2 \beta \mu_0 \theta \frac{V^2}{L^3} \quad (12)$$

where  $\theta = N_c/N_T \exp -\epsilon_T/kT$  and  $\epsilon_T$ —the energy position of the trap level.

Having in mind the previous consideration and the shape of the trap level distribution, we may try to interpret the current-voltage characteristics presented in Figs. 1–5. Curves presented in the graphs 1 and 4 correspond to the filling of the 0.2 eV maximum. By analogy, it may be stated that the curve in Fig. 2 is connected with the same maximum too.

The comparison of the curves of Figs. 2 and 3 suggest that the dependence of the photocurrent on voltage may be sometimes quite different from that of the dark current, though sometimes this difference is not very prominent (Figs. 4 and 5). The differences in the shape of the curves shown in Figs. 4 and 5 originate probably in fact that the curve on Fig. 5 is better described by Eqs. (4) or (5) than Eq. (2). It can be seen from Figs. 2 and 5 that straight lines with slope 2 may be observed. In such a case one may expect, especially in the high voltage range, that Eq. (12) is applicable. To verify the above, a mobility  $\mu[\mu = \mu_0 \theta]$  has been calculated. The calculation has been done by means of the data obtained from Fig. 2. The values obtained were unreasonably low, of the order of  $10^{-14} \text{ cm}^2/\text{V s}$ .

The mobility may be also calculated for the current and voltage values taken from Figs. 1 and 2 corresponding to the parts of the characteristic curves with the greatest slopes  $n$ . The calculations were performed with the assumption of the applicability of Eq. (2). Taking  $T_c/T = 8$ ,  $N_c = 10^{22} \text{ cm}^{-3}$  the values of  $\mu_0$  between  $10^{-10}$  and  $10^{-2} \text{ cm}^2/\text{V s}$  were evaluated when  $N_T$  was varied

between  $10^{16}$  and  $10^{17} \text{ cm}^{-3}$ . From the above we must come to the conclusion that  $\theta$  must be of the order  $10^{-4}$  or less, which is impossible because of the low value of  $\epsilon_T[\epsilon_T \leq 0.2 \text{ eV}]$ .

The discrepancy of the above two results can be explained by the inapplicability of Eq. 12 in that case. The lines with slope 2 are probably due to extrapolation of parts of the exponential curve by the power function. The second explanation is, that the saturation of the emission current of the electrode occurs in the highest fields.

One of the most important features of the observed voltage-current characteristics is that the slopes  $n$  are always less than  $T_c/T$ . It was pointed out by Muller<sup>10</sup> that for large and positive  $T_c$  the current-voltage characteristics is better described by the following equation:

$$I = \frac{e\mu_0 N_c V}{L} [\exp -\epsilon_l/kT] \left[ 1 + \frac{bV}{\rho_0 kT_c} \right]^{T_c/T} \quad (13)$$

The slope  $n$  calculated from Eq. (13) is:

$$n = \frac{d \ln I}{d \ln V} = 1 + \frac{T_c}{T} \left( \frac{aV}{1+aV} \right) \quad (14)$$

where

$$a = \frac{b}{\rho_0 kT_c}$$

Because almost always  $aV/(1+aV) < 1$  then  $n < (1 + T_c/T)$ . Only for the highest fields may  $n$  approach  $(1 + T_c/T)$ .

#### 4. Conclusions

The results presented are concerned both with the methods of determining the shape of the trap level distribution in dielectrics and the interpretation of the experimentally observed current-voltage characteristics.

The data obtained from the discussion of  $I=f(T, V)$  dependence are in accordance with the results of other methods and are



probably an interesting way of investigating trap density distribution.

The results presented above may suggest also that the evaluation of  $kT_c$  from the slope of the current-voltage characteristic and the estimation of the density of the trap levels from the value of the voltage corresponding to the sharp rise of the current may be sometimes erroneous because:

1. only some slopes can be related to the  $T_c/T + 1$  value,
2. the vertical lines on the  $\log I$ - $\log V$  characteristic may be related to the filling of a group of trap levels, but not to the filling of all trapping levels.

The above-mentioned considerations are applicable also to the calculation by the above-mentioned procedure of mobility value.

The author is much indebted to Prof. Dr. M. Kryszewski for stimulating discussion, and to Dr. McGhie for the help in the improvement of the manuscript.

#### REFERENCES

1. Tredgold, R. H., *Space Charge Conduction in Solids*, Elsevier Publ. Co, Amsterdam-New York-London, 1966.
2. Kallman, H. and Pope, M. *Nature* **186**, 31 (1960); *J. Chem. Phys.* **36**, 2482 (1961).
3. Mark, P. and Helfrich, W., *J. Appl. Phys.* **33**, 205 (1962); *Z. Phys.* **166**, 370 (1962); *Z. Phys.* **168**, 495 (1962); *Z. Phys.* **171**, 527 (1963).
4. Heilmayer, G. and Warfield, G., *J. Chem. Phys.* **38**, 163 (1963).
5. Silver, M., Mark, P., Olness, D., Helfrich, W., and Jarnagan, R. C., *J. Appl. Phys.* **33**, 1988 (1962).
6. Silver, M., Swicord, M., and Jarnagan, R. C., *J. Phys. Chem., Solids* **23**, 419 (1962).
7. Reucroft, P. J., Rudyj, O. N., and Labes, M. M., *J. Chem. Phys.* **39**, 1136 (1963).
8. Adolph, J., Baldinger, E., Czaja, W., and Granacher, J., *Phys. Lett. (Neth.)* **6**, 137 (1963); *Phys. Lett. (Neth.)* **8**, 244 (1964).
9. Rose, A., *Concepts in Photoconductivity*, Interscience Publ., New York-London, 1963; Rose, A., *Phys. Rev.* **97**, 1538 (1955).
10. Muller, R., *Solid State Electronics* **6**, 25 (1963).
11. Harnik, E., *J. Appl. Phys.* **36**, 3850 (1955).
12. Kurczewska, H., Private Communication.
13. Szymański, A., *Bull. Acad. Sci. Pol.* (in press).
14. Hill, E. and Goldsmith, G., *Phys. Rev.* **98**, 234 (1955).

15. Raman, R. and McGlynn, S. P. *H. Chem. Phys.* **40**, 515 (1964).
16. Szymański, A., *Acta Phys. Polon.* (in press).
17. Bassler, H., Becker, G., and Riehl, N., *Phys. Stat. Sol.* **15**, 347 (1966).
18. Thoma, P. and Vaugel, G., *Phys. Stat. Sol.* **16**, 663 (1966).
19. Riehl, N. and Thoma, P., *Phys. Stat. Sol.* **16**, 159 (1966).